JASA ARTICLE

A numerical extension of White's theory of P-wave attenuation to non-isothermal poroelastic media

Naddia D. Arenas Zapata,[1,2,3] Juan E. Santos,[1,4,5] Gabriela B. Savioli,[1] José M. Carcione,[4,6] and Jing Ba[4,a)]

[1]*Facultad de Ingeniería, Instituto del Gas y del Petróleo, Universidad de Buenos Aires, Buenos Aires C1127AAR, Argentina*

[2]*Facultad de Ciencias Astronómicas y Geofísicas, Universidad Nacional de La Plata, La Plata 1900, Argentina*

[3]*Consejo Nacional de Investigaciones Científicas y Técnicas, CONICET, Rosario S2000EZP, Argentina*

[4]*School of Earth Sciences and Engineering, Hohai University, Nanjing 211100, China*

[5]*Department of Mathematics, Purdue University, Indiana 47907-2067, USA*

[6]*Associate of National Institute of Oceanography and Applied Geophysics, Trieste 34010, Italy*

ABSTRACT:

Mesoscopic P-wave attenuation in layered, partially saturated thermo-poroelastic media is analyzed by combining the theories of Biot poroelasticity and Lord–Shulman thermoelasticity (BLS). The attenuation is quantified by estimating the quality factor Q. The mesoscopic attenuation effect, commonly referred to as wave-induced fluid flow (WIFF), is the process that converts fast compressional and shear waves into slow diffusive Biot waves at mesoscopic heterogeneities larger than the pore scale, but much smaller than the dominant wavelengths. This effect was first modeled in White's isothermal theory by quantifying the seismic response of a periodic sequence of planar porous layers that are alternately saturated with gas or water. This work presents a numerical extension of White's theory for the non-isothermal case in this type of sequence. For this purpose, an initial-boundary-value problem (IBVP) for the BLS wave propagation equations is solved using the finite element method, where the particle velocity field is recorded at uniformly distributed receivers. The quality factor is estimated using spectral-ratio and frequency-shift methods. The Q-estimates show that thermal effects influence the attenuation of the P-wave and the velocity dispersion compared to the isothermal case.

https://doi.org/10.1121/10.0024979

(Received 24 October 2023; revised 18 January 2024; accepted 5 February 2024; published online 16 February 2024)

[Editor: D. Keith Wilson] Pages: 1486–1491

I. INTRODUCTION

The theory of thermoelasticity describes the interaction between the deformation and temperature fields in elastic media. When an elastic source causes a deformation, it generates a temperature field and attenuation effects. This theory was one of the first to describe seismic attenuation in rocks (Lifshitz and Roukes, 2000; Zener, 1938; Carcione, 2022).

Biot's original theory described wave propagation in an isothermal poroelastic medium saturated with a single-phase viscous and compressible fluid (Biot, 1956a,b). A later work by Biot (1956c) presented a thermoelasticity model with a classical parabolic Fourier law of heat conduction. However, that theory gives unphysical solutions, such as infinite velocities at high frequencies. To overcome these drawbacks, Lord and Shulman (1967) formulated a hyperbolic differential equation by introducing Maxwell–Vernotte–Cattaneo (MVC) relaxation times into the heat equation. Thermoelasticity predicts the existence of an S-wave (shear wave) and two P-waves: one elastic, related to mechanical perturbations, and the other thermal, related to the temperature of the medium. Rudgers (1990) analyzed the coupled propagation of compressional and thermal waves as a function of frequency.

Sharma (2008) proposed a set of differential equations to analyze the propagation and attenuation of waves in non-isothermal fluid-saturated poroelastic media. Four waves are generated: two compressional waves (fast P1 and slow [Biot] P2), a slow thermal wave (T) compressional as well, and a shear wave (S). The two slow waves (P2 and T) have diffusive behavior at low frequencies that depends on viscosity and thermoelasticity constants. The T-wave is coupled with the two P-waves, and it is assumed that the temperatures in the solid and in the liquid are the same. The existence and uniqueness of initial-value-boundary problems (IBVPs) in open bounded domains under general boundary conditions was demonstrated in Santos *et al.* (2021).

Based on this theory, Carcione *et al.* (2019) developed a numerical algorithm to compute transient wave fields (seismograms). The work of Zener (1938) already contains the idea of conversion of P-mode waves into thermal modes, which can lead to dissipation of P-waves due to heterogeneities in the medium. This is similar to White's model (White *et al.*, 1975). White explains the attenuation of porous media due to inhomogeneities at the mesoscopic scale, where P-waves can be converted to the slow Biot mode.

Zener (1946) explored the concept of attenuation due to diffusion, including thermal, atomic, and magnetic diffusion

a)Email: jingba@188.com

https://doi.org/10.1121/10.0024979

as possible causes. Carcione and Picotti (2006) used the model proposed by White *et al.* (1975) to study the mesoscopic loss mechanism. This model considers a periodically stratified porous medium alternately saturated with water and gas to estimate the quality factor Q and velocity dispersion. Quality factor is an important seismic indicator for evaluating rock acoustic properties, which depend on mineral composition, fluid type, permeability, and porosity. The quality factor can be estimated by two methods: spectral ratio (SR) and frequency shift (FS). In the SR method, Q is calculated from the slope of the semilog relationship between the receiver amplitude spectrum and frequency, while the FS procedure exploits the correlation between the quality factor and the centroid frequencies at two receivers, with one receiver considered as the source for the other (Quan and Harris, 1997). Picotti *et al.* (2007) used a finite-element (FE) method to model the mesoscopic loss mechanism in a laminated porous medium alternately saturated with gas and water. They estimated the quality factor from synthetic time histories using both methods.

Santos *et al.* (2023) proposed a FE method for solving an IBVP for the Biot/Lord–Schulman equations, where absorbing boundary conditions were used at the artificial boundaries of the computational domain. This technique is applied here to investigate the mesoscopic loss effects in a non-isothermal poroelastic medium alternately saturated with gas and water. The novelty of this work lies in the analysis of the attenuation of P-waves caused by the mode conversion of T and P2 waves at gas-water interfaces and in its comparison with the attenuation due exclusively to the wave-induced fluid flow (WIFF) mechanism (WIFF-P1-P2 conversion) in the isothermal case. The effect of coupling a heat loss mechanism to White's thin-layer mesoscopic damping model is evaluated using FE numerical experiments.

II. GOVERNING EQUATIONS AND ALGORITHM

The porous medium under study is a periodic sequence of poroelastic layers alternately saturated with gas and water. The displacement vectors for the solid and fluid phases are expressed as $\mathbf{u}^s = (u_i^s)$ and $\mathbf{u}^f = (u_i^f)$, and the total displacement vector for both phases is $\mathbf{u} = (\mathbf{u}^s, \mathbf{u}^f)$. The stress tensor of the bulk material is denoted by $\boldsymbol{\sigma}(\mathbf{u}, \theta) = \sigma_{ij}(\mathbf{u}, \theta)$, where the subscript ij identifies the components and θ is the temperature increment above a reference temperature, θ_0. The fluid pressure is $p_f = p_f(\mathbf{u}, \theta)$, and the strain tensor is represented as $\boldsymbol{\varepsilon}(\mathbf{u}^s) = (\varepsilon_{ij}(\mathbf{u}^s))$. With these definitions, the constitutive equations are

$$\sigma_{ij}(\mathbf{u}, \theta) = 2\mu\, \varepsilon_{ij}(u^s) + \delta_{ij}(\lambda_u \nabla \cdot \mathbf{u}^s + B\nabla \cdot \mathbf{u}^f - \beta\, \theta), \tag{1}$$

$$-p_f(\mathbf{u}, \theta) = B\, \nabla \cdot \mathbf{u}^s + M\nabla \cdot \mathbf{u}^f - \beta_f \theta. \tag{2}$$

The quantities λ_u, M, and B are defined as $\lambda_u = \lambda + \alpha^2 M$, $\alpha = 1 - K_m/K_s$, $M = (\alpha - \phi/K_s + \phi/K_f)^{-1}$, and $B = \alpha M$, where λ and λ_u are the Lamé coefficient of the dry and saturated frames, respectively, K_s, K_m, and K_f denote the bulk moduli of the grains, solid and fluid, respectively, and ϕ is the rock porosity. Furthermore, μ is the dry-rock shear modulus, and β and β_f are positive coupling coefficients of thermoelasticity of the frame and fluid, respectively.

Biot's dynamical equation (Picotti *et al.*, 2007) is modified to take the temperature into account, as

$$\mathcal{P}\ddot{\mathbf{u}} + \mathcal{B}\dot{\mathbf{u}} - \mathcal{L}(\mathbf{u}, \theta) = \mathbf{f}, \tag{3}$$

where $\mathcal{L}(\mathbf{u}, \theta) = (\nabla \cdot \boldsymbol{\sigma}(\mathbf{u}, \theta), -\nabla p_f(\mathbf{u}, \theta))$, $\mathcal{P}$ is a positive definite matrix, and $\mathcal{B}$ is a nonnegative matrix given by

$$\mathcal{P} = \begin{pmatrix} \rho_b I & \rho_f I \\ \rho_f I & gI \end{pmatrix}, \quad \mathcal{B} = \begin{pmatrix} 0I & 0I \\ 0I & \dfrac{\eta}{\kappa} I \end{pmatrix}. \tag{4}$$

In Eq. (4), $\rho_b = (1 - \phi)\rho_s + \phi\rho_f$ is the bulk density, with ρ_s and ρ_f the densities of the grains and fluid, respectively, I is the identity matrix in $R^{d\times d}$, with $d = 1, 2, 3$, η is the fluid viscosity, κ is the permeability and $g = Sp_f/\phi$, where S is the tortuosity.

Sharma (2008) and Carcione *et al.* (2019) assumed thermal equilibrium between the solid and fluid phases, based on the external acoustic force: $\mathbf{f} = (\mathbf{f}^s, \mathbf{f}^f)$. The generalized heat equation is

$$\begin{aligned} &\tau\, c\, \ddot{\theta} + c\, \dot{\theta} - \nabla \cdot (\gamma \nabla\theta) + \beta\theta_0 \nabla \cdot \dot{\mathbf{u}}^s + \beta\theta_0 \nabla \cdot \dot{\mathbf{u}}^f \\ &\quad + \tau\beta\theta_0 \nabla \cdot \ddot{\mathbf{u}}^s + \tau\beta\theta_0 \nabla \cdot \ddot{\mathbf{u}}^f = -q, \end{aligned} \tag{5}$$

where $\gamma = (1 - \phi)\gamma_m + \phi\gamma_f$ is the bulk thermal conductivity coefficient, with γ_m and γ_f the thermal conductivity of the frame and fluid, respectively, c is the specific heat of the unit volume in the absence of deformation, τ is a MVC relaxation time, and q is a heat source. We can assume thermal equilibrium, under the conditions that the interstitial heat transfer coefficient between the solid and the fluid is very large and the ratio of pore surface area to pore volume is sufficiently large. Here, we consider β, β_f, γ, and c as strictly positive parameters obtained from experiments or from a specific theoretical model.

Note that we add the temperature terms in Biot's dynamic equation [Eq. (3)] through the operator $\mathcal{L}(\mathbf{u}, \theta)$ and the constitutive relations in Eqs. (1) and (2), and we also consider the influence of the velocities and accelerations of the solid and fluid phases on the heat equation [Eq. (5)]. In both equations, the thermal coupling coefficients β and β_f are used.

To solve the initial boundary value problem for the Biot/Lord–Schulman equations [Eqs. (3)–(5)], Santos *et al.* (2023) proposed and analyzed a FE procedure. Next, the problem is formulated in two dimensions (2D), with natural reduction to the 1D case and natural extension to the 3D case. It considers thermal equilibrium in an open bounded domain, Ω, with a piecewise smooth boundary, Γ, and a time interval, $J = (0, T)$. The problem is formulated as follows: Find $(\mathbf{u}, \theta)$, satisfying Eqs. (3)–(5), such that

$$\mathbf{u}(x, 0) = \mathbf{u}^0 = (\mathbf{u}^{0,s}, \mathbf{u}^{0,f}), \quad \dot{\mathbf{u}}(x, 0) = \mathbf{u}^1 = (\mathbf{u}^{1,s}, \mathbf{u}^{1,f}), \quad x \in \Omega, \tag{6}$$

$$\theta(x,0)=\theta^0, \quad \dot{\theta}(x,0)=\theta^1, \quad x\in\Omega, \tag{7}$$

with the absorbing boundary conditions

$$-\mathcal{G}_\Gamma(\mathbf{u},\theta)=\mathcal{D}\mathcal{S}(\dot{\mathbf{u}}), \tag{8}$$

$$-\gamma\nabla\theta\cdot\boldsymbol{\nu}=\tau c v_\theta\dot{\theta} \quad x\in\Gamma, \quad t\in J, \tag{9}$$

where

$$\mathcal{G}(\mathbf{u},\theta)=(\boldsymbol{\sigma}\boldsymbol{\nu}\cdot\boldsymbol{\nu},\boldsymbol{\sigma}\boldsymbol{\nu}\cdot\boldsymbol{\chi},p_f)(\mathbf{u},\theta),$$
$$\mathcal{S}(\dot{\mathbf{u}})=\left(\dot{\mathbf{u}}^s\cdot\boldsymbol{\nu},\dot{\mathbf{u}}^s\cdot\boldsymbol{\chi},\dot{\mathbf{u}}^f\cdot\boldsymbol{\nu}\right). \tag{10}$$

In Eqs. (8)–(10), $\boldsymbol{\nu}$ and $\boldsymbol{\chi}$ are given as the unit vector outer normal and the unit vector tangent on Γ oriented counterclockwise. Equation (8) defines an absorbing boundary condition derived in Santos *et al.* (1988), with $\mathcal{D}$ being a positive definite matrix. Furthermore, $v_\theta=\sqrt{\gamma/(\tau c)}$ is the heat speed (e.g., Carcione *et al.*, 2020). In the 1D case, the formulation of the IBVP in Eqs. (3)–(10) remains valid, omitting the tangent vector $\boldsymbol{\chi}$, while in the 3D case, two tangents $(\boldsymbol{\chi}_1,\boldsymbol{\chi}_2)$ must be considered.

The IVBP solution provides the seismic response in the form of displacements of the solid and fluid phases and temperature, which are recorded to observe and quantify the attenuation effects of the P-waves. In the FE method, globally continuous bilinear polynomials are used for spatial discretization to represent solid and fluid displacements and temperature. In addition, an explicit temporal discretization is applied, which imposes a stability constraint (Santos *et al.*, 2023). In the numerical experiments, the IBVP is solved in a 1D interval to model the wave propagation and quantify the attenuation effects.

III. ESTIMATION OF THE ATTENUATION

The SR and FS methods are used to estimate the quality factor. The first computes the ratio of the spectral amplitudes $A(f,r_s)$ and $A(f,r_t)$ between two receivers, r_s and r_t, where r_s is considered as the source and r_t as the receiver. The method is based on the following equation (Mavko *et al.*, 2003):

$$\ln\left[\frac{A(f,r_s)}{A(f,r_t)}\right]=\frac{\pi(d_t-d_s)}{c_pQ}f, \tag{11}$$

where d_s and d_t are source-receiver distances and c_p is the average P-wave phase velocity. Therefore, Q is computed from the slope of the semilog relationship in Eq. (11).

The FS method introduced by Quan and Harris (1997) relates the quality factor Q with the centroid frequencies at source and receiver defined as

$$f_j=\frac{\int_0^\infty fA(f,r_j)df}{\int_0^\infty A(f,r_j)df}, \quad j=s,t. \tag{12}$$

TABLE I. Frame properties.

Property	Value
Grain bulk modulus, K_s	37 GPa
Density, ρ_s	2650 kg/m^3
Frame bulk modulus, K_m	8 GPa
Shear modulus, μ_m	9.5 GPa
Porosity, ϕ	0.3
Permeability, κ	1 darcy

The method is based on the fact that a wave that propagates through a medium loses high frequencies, and then the centroid decreases. This effect can be measured by the resulting downshift, denoted as $\Delta f=f_s-f_t$, where f_s and f_t are the source and receiver centroid frequencies. Furthermore, $A(f,r_s)$ is approximated by a Gaussian curve with a variance, σ_s^2, and Q is obtained from the following relationship:

$$\pi\frac{(d_t-d_s)}{c_pQ}=\frac{(f_s-f_t)}{\sigma_s^2}. \tag{13}$$

IV. NUMERICAL RESULTS

Numerical experiments were performed to analyze the attenuation behavior and to estimate the quality factor in a partially saturated thermo-poroelastic sample. The medium consists of alternating layers of equal thickness saturated with gas and water. The frame properties are listed in Table I, the fluid properties in Table II, and the thermal parameters in Table III. The numerical experiments consist of finding approximate solutions of IBVPs for the Biot/Lord–Shulman equations using the FE method in open domains that are intervals, with absorbing boundary conditions at the boundaries. Then the FS and SR methods are applied to estimate the quality factor.

In all the examples, the medium, initially at rest, was excited by a dilatation point source of time history,

$$g(t)=-16f_0^2(t-t_0)e^{-8f_0^2(t-t_0)^2}, \tag{14}$$

where $t_0=1.25/f_0$ and f_0 is the dominant frequency.

The objective of experiment 1 is to analyze the propagation and wave amplitude behavior in both the coupled and uncoupled elastic-thermal cases in order to estimate the quality factor. In the coupled case, the effects of temperature are taken into account, which means that the thermoelasticity

TABLE II. Fluid properties.

Property	Value
Fluid bulk modulus (water), K_f	2.25 GPa
Density (water), ρ_f	1040 kg/m^3
Viscosity (water), η_f	0.003 Pa · s
Fluid bulk modulus (gas), K_f	0.012 GPa
Density (gas), ρ_f	78 kg/m^3
Viscosity (gas), η_f	0.000015 Pa · s

https://doi.org/10.1121/10.0024979

TABLE III. Thermal parameters.

Parameter	Value
Thermoelasticity coefficient, β_f	50 000 kg/(m s^2 K)
Bulk specific heat, c	820 kg/(m s^2 K)
Thermoelasticity coefficient, β	90 000 kg/(m s^2 K)
Absolute temperature, T_0	300 K
Thermal conductivity, γ	4.5×10^6 kg/m^3
Relaxation time, τ	1.5×10^{-2} s

coefficients β and β_f are not zero. This experiment considers an interval of $\Omega = (0, 400\,\text{m})$, consisting of periodic layers of thickness 20 cm alternately saturated with gas and water, which is discretized with a uniform mesh of size $h = 0.2$ m. The medium is excited with a dilatation point source of dominant frequency $f_0 = 77$ Hz located at $x_s = 4$ m. Four receivers (r1, r2, r3, and r4) are placed at $x_1 = 70$ m, $x_2 = 100$ m, $x_3 = 130$ m, and $x_4 = 160$ m. The time histories of the frame particle velocities are recorded at the receivers.

Experiment 2 quantifies the quality factor and the amplitude spectrum in two coupled cases with different layer thicknesses. Both cases consider an interval of $\Omega = (0, 400\,\text{m})$ with periodic layers alternately saturated with gas and water. The medium is excited with a source located at 4 m, and the frame particle velocities are recorded at five receivers located at $x_1 = 70$ m, $x_2 = 100$ m, $x_3 = 130$ m, $x_4 = 160$ m, and $x_5 = 190$ m. The first case has periodic layers of 15 cm thickness, and the source dominant frequency is $f_0 = 140$ Hz, while the second case considers layers of 30 cm and a source of dominant frequency $f_0 = 34$ Hz.

To analyze the amplitude damping of a wave propagating in a partially saturated thermo-poroelastic medium, we compare the results with White's isothermal theory. White's model describes dissipation in a medium composed of periodic layers saturated with gas and water. The dissipation is due to the interaction generated by the presence of two fluids with different compressibilities (White *et al.*, 1975). Figure 1 shows the inverse quality factor as a function of frequency for three thicknesses (15, 20, and 30 cm). The minimum value of the quality factor for all thicknesses is 28.

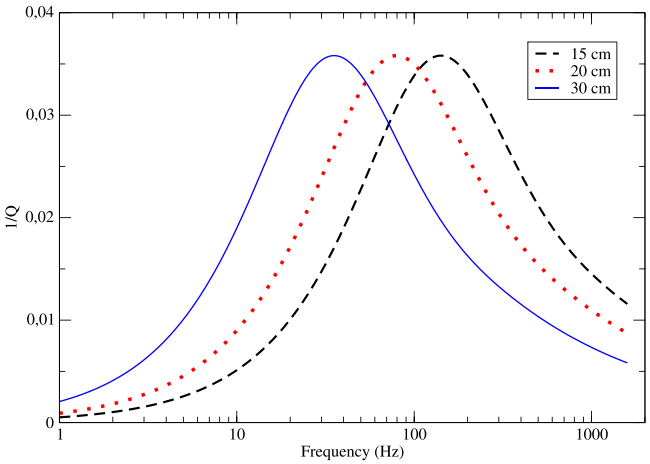

FIG. 1. (Color online) Inverse quality factor Q for a water and gas saturated Biot sandstone corresponding to three layer thicknesses (15, 20, and 30 cm).

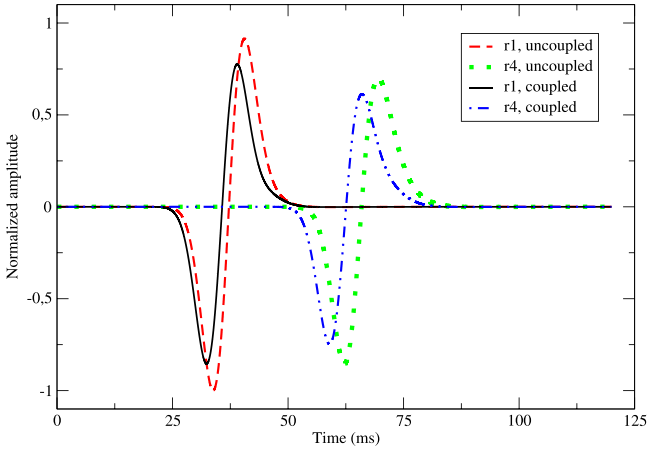

FIG. 2. (Color online) Time histories of the frame particle velocity recorded at 70 m (receiver r1) and 160 m (receiver r4), considering (coupled) and neglecting (uncoupled) thermal effects. The experiment considers an interval of $\Omega = (0, 400\,\text{m})$, consisting of periodic layers of thickness 20 cm alternately saturated with gas and water (experiment 1).

Figure 2 shows the time histories of the frame particle velocity at receivers r1 and r4 for both the uncoupled and coupled cases in experiment 1, with the amplitudes normalized to the maximum amplitude of the signal at r1 in the uncoupled case. This normalization provides a better representation of the relative changes in wave propagation and attenuation between the two cases. This figure shows that the coupled case exhibits faster wave propagation and lower amplitude due to the inclusion of temperature effects in addition to the WIFF described by White's theory.

Figure 3 shows the normalized amplitude spectra at receivers r1 and r4 in experiment 1. This graph, like Fig. 2, shows lower amplitude spectra and higher attenuation when temperature effects are included (coupled case).

Figure 4 illustrates the normalized amplitude spectra of the four receivers in the coupled case of experiment 1. The amplitude spectrum of the waves decreases as the

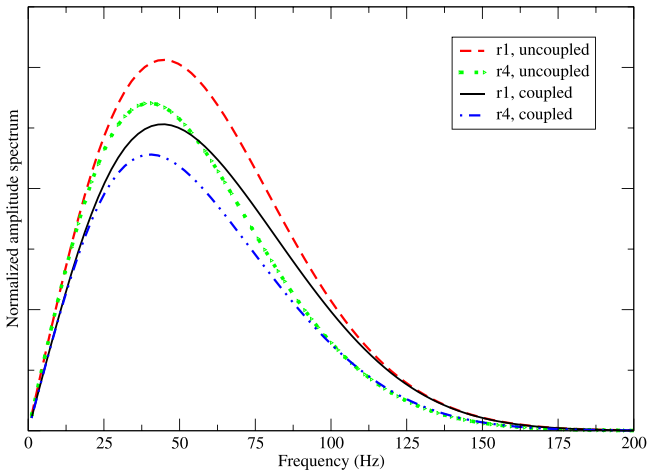

FIG. 3. (Color online) Amplitude spectra corresponding to the time history recorded at 70 m (receiver r1) and 160 m (receiver r4), considering (coupled) and neglecting (uncoupled) thermal effects (experiment 1).

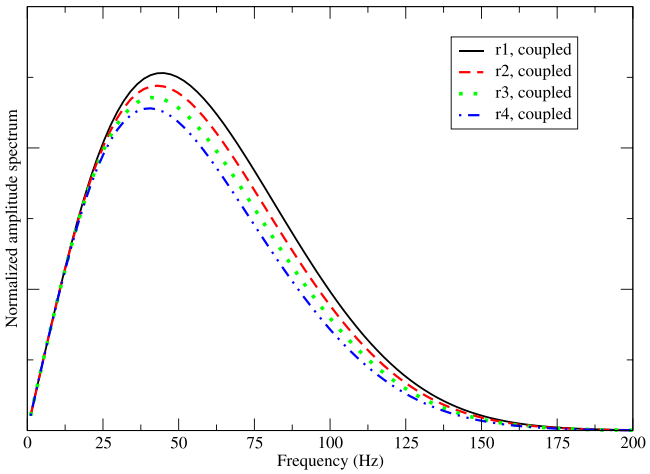

FIG. 4. (Color online) Amplitude spectra corresponding to the time history recorded at 70 m (receiver r1), 100 m (receiver r2), 130 m (receiver r3), and 160 m (receiver r4), considering (coupled) thermal effects (experiment 1).

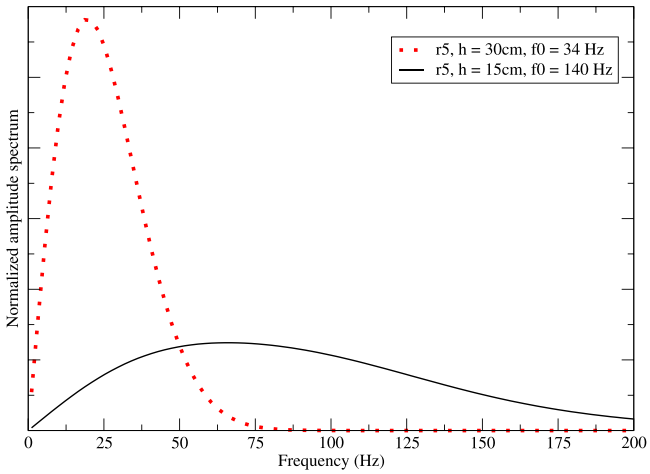

FIG. 5. (Color online) Amplitude spectra corresponding to the time history recorded at 190 m (receiver r5), including thermal effects, for layer thicknesses 15 and 30 cm. The experiment considers an interval of $\Omega = (0, 400\,\text{m})$ consisting of periodic layers alternately saturated with gas and water (experiment 2).

distance between the receivers and the source increases, due to the loss of energy by mode conversions.

Table IV shows the estimation of the quality factor by using the SR and FS methods in the coupled and uncoupled cases of experiment 1 and considering the four receivers. As expected, the results obtained with the two methods in the uncoupled case are similar to the theoretical value obtained with White's theory, ($Q = 28$) at 77 Hz, and higher than the estimates for the coupled case. This shows that when temperature effects are taken into account, the attenuation of the wave is higher, so that the quality factor decreases.

Finally, in experiment 2, the influence of layer thickness is analyzed in the coupled case. Figure 5 shows that the amplitude spectrum computed in the receiver r5 for layer thickness 30 cm is higher than that obtained for layer thickness 15 cm. This is due to the fact that there is less mode conversion and, consequently, larger amplitude and less attenuation, when the wave propagates through a larger layer thickness.

Table V compares the estimated quality factors for layer thicknesses 15 and 30 cm in the coupled case. As expected, the Q-estimates reported in Table V are lower than the theoretical value of White, due to the temperature effects. Q-values for a layer thickness of 30 cm are higher than those of 15 cm, since there is less mode conversion. Thus, for 30 cm, we have a larger amplitude spectrum and less attenuation than for 15 cm.

TABLE IV. Estimated Q computed with the SR and FS methods.[a]

		Coupled		Uncoupled	
Source	Receiver	SR coupled	FS coupled	SR uncoupled	FS uncoupled
r1	r2	24.53	23.9	29.17	27.47
r1	r3	24.51	24.12	28.48	27.1
r1	r4	24.07	23.91	28.72	27.68
r2	r3	24.53	24.35	27.79	26.72
r2	r4	23.84	23.91	28.49	27.78
r3	r4	23.15	24.46	29.22	28.85

[a]Shown are results for the coupled and uncoupled cases in experiment 1. SR, spectral ratio; FS, frequency shift.

V. CONCLUSIONS

Wave propagation in a partially saturated thermo-poroelastic medium is studied by numerically solving an IBVP for the Biot/Lord–Shulman equations in periodic sequences of poroelastic layers alternately saturated with gas and water. The medium is excited with a dilatational point source, and the particle velocity is recorded at equally spaced receivers. Furthermore, the same experiment is performed using the classical isothermal Biot's theory. The quality factor Q is estimated using the SR and FS methods.

The first experiment compares the results of the non-isothermal (Biot/Lord–Shulman, coupled) and isothermal (Biot, uncoupled) cases for a periodic sequence of layer thickness 20 cm and a source dominant frequency of 77 Hz,

TABLE V. Estimated Q for 15 and 30 cm thickness computed with the SR and FS methods.[a]

		15 cm		30 cm	
Source	Receiver	SR	FS	SR	FS
r1	r2	24.57	24.43	26.50	27.24
r1	r3	23.74	23.91	26.71	26.52
r1	r4	23.75	24.24	26.83	26.37
r1	r5	23.58	24.41	26.88	26.54
r2	r3	22.94	22.84	26.94	26.41
r2	r4	23.35	23.58	26.99	26.54
r2	r5	23.25	23.83	27.01	26.93
r3	r4	23.75	23.70	27.04	26.68
r3	r5	23.41	23.70	27.05	27.20
r4	r5	23.07	23.02	27.06	27.06

[a]Shown are results from the coupled case in experiment 2. SR, spectral ratio; FS, frequency shift.

which corresponds to the frequency attenuation peak of White's theory. The results show a higher attenuation (i.e., lower Q) in the coupled case caused by the combination of the WIFF mechanism with the conversion of P-waves into thermal waves. In the uncoupled case, the numerical Q-estimates agree very well with the value predicted by White's theory.

The second experiment analyzes the mesoscopic loss mechanism in the coupled case, considering layer thicknesses of 15 and 30 cm with associated dominant frequencies of 140 and 34 Hz, respectively. As expected, thicker layers yield greater Q-values and less attenuation due to less mode conversions at gas-water interfaces.

The results obtained in both experiments show that P-wave attenuation increases when thermal effects are taken into account.

ACKNOWLEDGMENTS

This work was partially funded by ANPCyT, Argentina (Contract No. PICT 2015 1909) and the Universidad de Buenos Aires (Contract No. UBACyT 20020190100236BA).

AUTHOR DECLARATIONS

Conflict of Interest

The authors declare that the research was conducted in the absence of any commercial or financial relationships that could be construed as a potential conflict of interest.

DATA AVAILABILITY

The data that support the findings of this study are available from the corresponding author upon reasonable request.

Biot, M. A. (**1956a**). "Theory of propagation of elastic waves in a fluid saturated porous solid. I. Low frequency range," J. Acoust. Soc. Am. **28**, 168–178.

Biot, M. A. (**1956b**). "Theory of propagation of elastic waves in a fluid saturated porous solid. II. Higher frequency range," J. Acoust. Soc. Am. **28**, 179–191.

Biot, M. A. (**1956c**). "Thermoelasticity and irreversible thermodynamics," J. Appl. Phys. **27**, 240–253.

Carcione, J. M. (**2022**). *Wave Fields in Real Media: Theory and Numerical Simulation of Wave Propagation in Anisotropic, Anelastic, Porous, and Electromagnetic Media*, 4th ed., revised and extended (Elsevier, Amsterdam).

Carcione, J. M., Cavallini, F., Wang, E., Ba, J., and Fu, L. Y. (**2019**). "Physics and simulation of wave propagation in linear thermoporoelastic media," J. Geophys. Res., [Solid Earth] **124**, 8147–8166, https://doi.org/10.1029/2019JB017851.

Carcione, J. M., Gei, D., Santos, J. E., Fu, L. Y., and Ba, J. (**2020**). "Canonical analytical solutions of wave-induced thermoelastic attenuation," Geophys. J. Int. **221**, 835–842.

Carcione, J. M., and Picotti, S. (**2006**). "P-wave seismic attenuation by slow-wave diffusion: Effects of inhomogeneous rock properties," Geophysics **71**, O1–O8.

Lifshitz, R., and Roukes, M. L. (**2000**). "Thermoelastic damping in micro- and nanomechanical systems," Phys. Rev. B **61**, 5600–5609.

Lord, H., and Shulman, Y. S. (**1967**). "A generalized dynamical theory of thermoelasticity," J. Mech. Phys. Solids **15**, 299–309.

Mavko, G., Mikerji, T., and Dvorkin, J. (**2003**). *The Rock Physics Handbook, Tools for Seismic Analysis in Porous Media* (Cambridge University Press, Cambridge, UK).

Picotti, S., Carcione, J. M., Rubino, J., and Santos, J. E. (**2007**). "P-wave seismic attenuation by slow-wave diffusion: Numerical experiments in partially saturated rocks," Geophysics **72**, N11–N21.

Quan, Y., and Harris, J. M. (**1997**). "Seismic attenuation tomography using the frequency shift method," Geophysics **62**, 895–905.

Rudgers, A. J. (**1990**). "Analysis of thermoacoustic wave propagation in elastic media," J. Acoust. Soc. Am. **88**, 1078–1094.

Santos, J. E., Carcione, J. M., and Ba, J. (**2021**). "Existence and uniqueness of solutions of thermo-poroelasticity," J. Math. Anal. Appl. **499**, 124907.

Santos, J. E., Carcione, J. M., Savioli, G. B., and Ba, J. (**2023**). "Wave propagation in thermo-poroelasticity: A finite-element approach," Geophysics **88**, WA161–WA175.

Santos, J. E., Douglas, J., Jr., Morley, M. E., and Lovera, O. M. (**1988**). "Finite element methods for a model for full waveform acoustic logging," IMA J. Numer. Anal. **8**, 415–433.

Sharma, M. D. (**2008**). "Wave propagation in thermoelastic saturated porous medium," J. Earth Syst. Sci. **117**, 951–958.

White, J. E., Mikhaylova, N. G., and Lyakhovitskiy, F. M. (**1975**). "Low-frequency seismic waves in fluid saturated layered rocks," J. Acoust. Soc. Am. **57**(S30), S30–S659.

Zener, C. (**1938**). "Internal friction in solids ii. general theory of thermoelastic internal friction," Phys. Rev. **53**, 90–99.

Zener, C. (**1946**). *Anelasticity of Metals*, Pub. No. 1992 (American Institute of Mining and Metallurgical Engineers, New York).